Desalination and Water Treatment
www.deswater.com
doi: 10.1080/19443994.2015.1016460

57 (2016) 7302–7311
April

Taylor & Francis
Taylor & Francis Group

Luffa acutangula peel as an effective natural biosorbent for malachite green removal in aqueous media: equilibrium, kinetic and thermodynamic investigations

Hon Wei Ng, Lai Yee Lee*, Wei Leong Chan, Suyin Gan, Nishanth Chemmangattuvalappil

Department of Chemical and Environmental Engineering, The University of Nottingham Malaysia Campus, Jalan Broga, 43500 Semenyih, Selangor, Malaysia, Tel. +603 8924 8172; Fax: +603 8924 8017; email: lai-yee.lee@nottingham.edu.my (L.Y. Lee)

Received 31 October 2014; Accepted 29 January 2015

ABSTRACT

Luffa acutangula peel (LAP) was evaluated as an inexpensive natural biosorbent for the removal of malachite green (MG), a cationic dye, in batch mode. The effects of process parameters including initial pH, dosage, initial concentration, temperature and contact time on MG biosorption were assessed. Experimental data were analysed by the Langmuir, Freundlich, Temkin and Dubinin–Radushkevich models. The results showed that MG biosorption was well represented by the Langmuir model with a maximum sorption capacity of 69.64 mg/g. The pseudo-first-order and pseudo-second-order kinetic models were used to establish the biosorption kinetic. A good correlation of data with the pseudo-second-order model suggested the involvement of chemisorption in the process. Further kinetic analysis indicated intraparticle diffusion as one of the rate limiting steps. The biosorption process was endothermic ($\Delta H^\circ = 0.332$–12.64 kJ/mol) and spontaneous ($\Delta G^\circ = -20.81$ to -14.28 kJ/mol). Overall, the findings suggested that LAP can be an effective biosorbent for the removal of MG in aqueous solution.

Keywords: Luffa acutangula peel; Malachite green; Equilibrium; Kinetic; Thermodynamic

1. Introduction

Rapid industrialisation and urbanisation have caused severe water pollution in recent years. In particular, the contamination of water resources by synthetic dyes is a major global concern because of their detrimental effects on human beings and other organisms [1]. Dyes are used in various industries as colouring agent for products such as textile, cosmetic, paper, food, pharmaceutical and plastic. More than 700,000 tons of over 10,000 types of synthetic dyes are produced yearly to support these industries. Of this amount, typically 10–15% is released into the environment through wastewater generation and disposal [2,3]. Synthetic dyes are designed to be resistant against heat, sunlight, chemical and biological materials, hence the treatment of dye-bearing wastewater is very difficult [4].

Malachite green (MG) is a cationic dye used widely to colour silk, wool, cotton, leather, paper and food [5]. It belongs to the triphenylmethane group, and is also used as antiseptic and fungicidal for humans, and as antiparasitical, antibacterial and

*Corresponding author.

antifungal in aquaculture and commercial fish hatchery industries [6,7]. Despite its extensive usage, MG is highly toxic and can cause health problems such as damages to nervous system, brain and liver when ingested [8,9]. It is also known to be carcinogenic and mutagenic [5,10]. Apart from causing undesirable colour effect, the presence of MG in the hydrosphere reduces photosynthesis by obstructing light transmission and thus, adversely impacts aquatic life. Therefore, it is necessary to remove MG from industrial wastewater prior to discharge into the environment.

The technologies available for the remediation of dye contaminated wastewater include coagulation, flocculation, biological treatment, membrane filtration, ion exchange and oxidation. These technologies, however, suffer from high operating and capital costs, waste disposal issue resulting from sludge formation and ineffectiveness in treating wastewater with low dye concentration [11]. Adsorption technology has been employed for the removal of toxic pollutants from the water environment for the past two decades [10,12,13]. It is considered as one of the most efficient and versatile technology which results in complete eradication of pollutants from the wastewater [14,15]. This technology is easier to design and operate, hence requires lesser investment cost as compared with conventional biological treatment method. In addition, it does not leave behind any toxic by-products [15]. Adsorption is economically viable and cost effective when inexpensive adsorbents (or biosorbents) prepared from agricultural residues are used [16].

Agricultural residues are gaining increasing attention as potential resources for biosorbent preparation due to their low cost, abundant availability, renewability and eco-friendly nature [17,18]. The re-use of these residues in wastewater treatment can help to alleviate problems pertaining to solid waste disposal in agricultural industry [10,19]. The high efficiency of agricultural-derived biosorbents in water pollution control has been linked to various uptake mechanisms such as ion exchange, chelation, complexation, physical adsorption and surface precipitation [20]. Some of the biosorbents tested for dye removal include sugarcane bagasse [14], lotus leaves [21], pine sawdust [22], peanut husk [23], okra seeds [24] and pineapple leaf [25]. *Luffa acutangula*, or ridge gourd, is widely grown in Malaysia and other tropical countries to be used as culinary vegetable and scrubbing sponge. It is also used as antioxidant, antidiabetic and anticancer agent [26]. Because of its widespread use, the waste peel is readily available as a viable biosorbent for the removal of MG.

The present research investigates the potential use of *Luffa acutangula* peel (LAP) as biosorbent for MG removal from aqueous solutions. To date, there is a lack of published data on its sorption ability for MG. Batch parameters influencing the dye biosorption such as dosage, contact time, initial pH, initial dye concentration and temperature were investigated. The equilibrium, kinetic and thermodynamic parameters of the process were also evaluated.

2. Materials and methods

2.1. Biosorbent preparation

L. acutangula was obtained from a local market and washed several times with distilled water to remove dirt. The outer layer of the plant was peeled, cut and dried at 60°C for 24 h in a forced-convection oven (Memmert). The dried peels were ground and sieved to obtain particles of sizes between 100 and 125 μm. Finally, the particles were stored in a desiccator for usage as biosorbent in further experiments.

2.2. Point of zero charge of biosorbent

The point of zero charge (*PZC*) of the biosorbent was determined based on the solid addition method [27]. First, 20 mL of 1 mol/L KNO_3 solution was added into a series of conical flasks. The initial pH of the solutions was adjusted from 2 to 11 by dosing with either 0.1 mol/L NaOH or 0.1 mol/L HCl. Then, 0.2 g of biosorbent was added to each flask. The mixtures were agitated in a water bath shaker (Protect) for 24 h at 25°C. Thereafter, the final pH of the solutions was measured. The *PZC* was determined from the plot of pH change vs. initial pH.

2.3. Preparation of dye solutions

The dye used, MG ($C_{23}H_{25}ClN_2$, 364.9 g/mol), was purchased from Sigma-Aldrich. It was used without any purification. A stock solution of 1,000 mg/L MG was prepared by dissolving 1 g of dye powder in 1 L of distilled water. Experimental solutions of different dye concentrations were prepared by successive dilution of the stock solution with distilled water. The MG concentration was determined by UV–vis spectrophotometer (Perkin-Elmer Lambda 25) at the maximum absorbance of 615 nm. The calibration curve with high correlation (>0.999) was obtained by measuring the absorbance of known concentrations of dye solutions.

2.4. Batch biosorption experiments

The biosorption experiments were conducted using a series of conical flasks (100 mL capacity) filled with

50 mL dye solution of initial concentration 50 mg/L. The flasks were agitated in a water bath shaker at 125 rpm. The effect of initial pH on MG removal was investigated in the pH range of 2–10. Prior to addition of biosorbent, the pH of the solutions was adjusted to the desired values by adding either 0.1 mol/L HCl or 0.1 mol/L NaOH. To determine the influence of LAP dosage on MG removal, various amounts of biosorbent (0.1–2.0 g) were used. Different initial MG concentrations (30–600 mg/L) were used when investigating the impact of concentration on the dye biosorption. The effect of temperature was assessed at temperatures varying from 30 to 50˚C. All experiments were conducted for 3 h until equilibrium was attained, as determined from a preliminary study. Thereafter, the biosorbent was separated from solutions by centrifugation at 5,000 rpm for 10 min. The dye concentration in the supernatant was determined by UV–vis spectrophotometer.

The biosorption kinetic was assessed by contacting 0.8 g biosorbent with 200 mL MG solution of initial concentration 30 mg/L at 30˚C and 125 rpm. At predefined time intervals, sample solutions were collected, centrifuged and analysed for remaining dye concentration. The procedures were repeated with different initial concentrations (40 and 50 mg/L).

All experiments were performed at least three times to ensure accurate, reliable and reproducible data, and the results are reported as mean values [28]. Control experiments (without biosorbent) were carried out concurrently to ensure that MG sorption on the glass wall was negligible. The experiments were performed at the natural pH of solution, except for the pH study.

3. Results and discussion

3.1. Effect of biosorbent dosage

The effect of biosorbent dosage on the removal of MG is shown in Fig. 1. The percentage removal of MG increased from 57.12 to 92.14% with an increase in LAP dosage from 2 to 8 g/L. It remained nearly constant at this plateau (92.14%) as the biosorbent dosage was increased beyond 8 g/L. The increasing trend might be attributed to the higher number of available sorption sites provided by the higher quantity of biosorbent per fixed volume of solution [29]. At dosage above 8 g/L, the availability of sorption sites did not have any significant effects on MG removal. Therefore, the optimum dosage selected for the process was 8 g/L and this was employed in subsequent experiments.

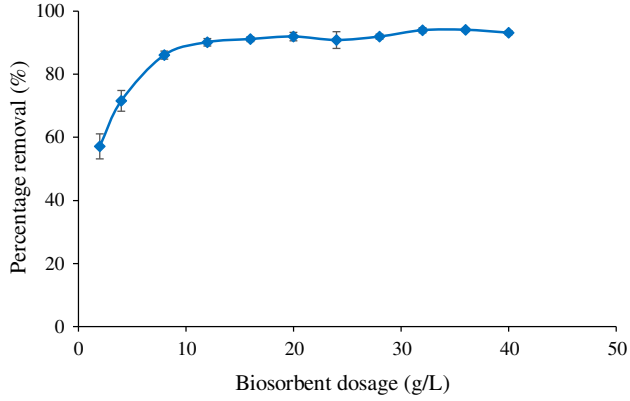

Fig. 1. Effect of LAP dosage on the percentage removal of MG dye.

3.2. Effect of initial pH

The pH of the solution is a significant parameter affecting the biosorption of MG since the biosorbent surface charge and chemical structure of the dye are pH-dependent [30]. The plot for the effect of initial pH on percentage removal of MG is depicted in Fig. 2(a). As can be seen, the percentage MG removal

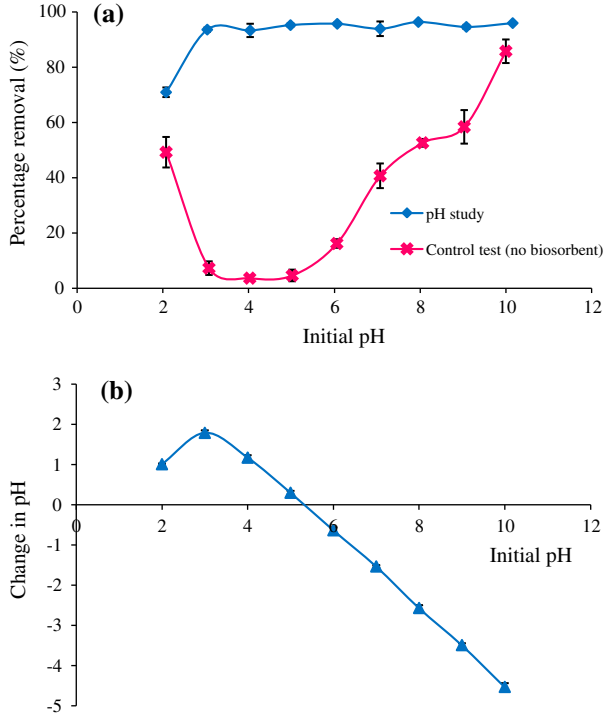

Fig. 2. Effect of initial pH on percentage MG removal by LAP (a) and *PZC* plot for LAP (b).

increased from 70.90 to 93.57% with increasing pH from 2 to 3, thereafter it remained nearly constant with further increase in pH. Similar results have been observed for the biosorption of MG on bagasse fly ash [31] and degreased coffee bean [32].

The effect of pH on the removal of the dye can be interpreted according to the *PZC* of the biosorbent [28]. The *PZC* of LAP determined by the solid addition method was approximately 5.3 (Fig. 2(b)). Theoretically, at pH lower than the *PZC*, the biosorbent surface is positively charged while at pH greater than the *PZC*, it is negatively charged. Since MG is a cationic dye, positive charge on LAP will be unfavourable for the dye biosorption. Fig. 2(a) shows that the percentage removal of MG between pH 3 and 5.3 is relatively high (about 94%) even though the biosorbent surface charge is anticipated to be positive. This suggests that the biosorption of MG onto LAP might not be governed mainly by coulombic or electrostatic interaction [33,34]. However, the influence of pH on dye removal can be explained on the basis of competitive sorption between H^+ ions and MG cations. At low pH (pH < 3), the lower percentage MG removal was due to H^+ ions competing with dye cations for same active sites on LAP, thereby inhibiting the biosorption of the dye [35]. As the pH increased from pH 2 to 3, weaker competitive biosorption of H^+ ions resulted in the increase of MG removal.

The plot of the control test carried out using blank dye solutions (without LAP) is also shown in Fig. 2(a). It can be seen that MG removal occurred at pH < 3 and pH > 5, although no biosorbent was present. The dye lost resulting solely from pH change might be caused by structural changes, chemical reactions or dissolutions occurring on the dye molecules [30,31]. It has been reported that formation of MGH^{2+} and alkaline fading of MG were the main causes of dye loss at pH 2 and 10, respectively [36]. It can also be inferred from the control plot (Fig. 2(a)) that between pH 3 and 5, MG was stable and there was no significant dye removal by sorption on glass wall or other phenomena. The natural pH of MG solution was approximately 4 and at this pH, the dye molecules were stable. Therefore, subsequent biosorption experiments were carried out at this natural pH.

3.3. Biosorption equilibrium

Fig. 3 shows the influence of equilibrium concentration on the biosorption capacity of MG at 30, 40 and 50°C. The biosorption capacity increased with increasing dye concentration for all temperatures investigated. This trend could be attributed to increased driving force for mass transfer between liquid–solid phases as dye concentration was increased.

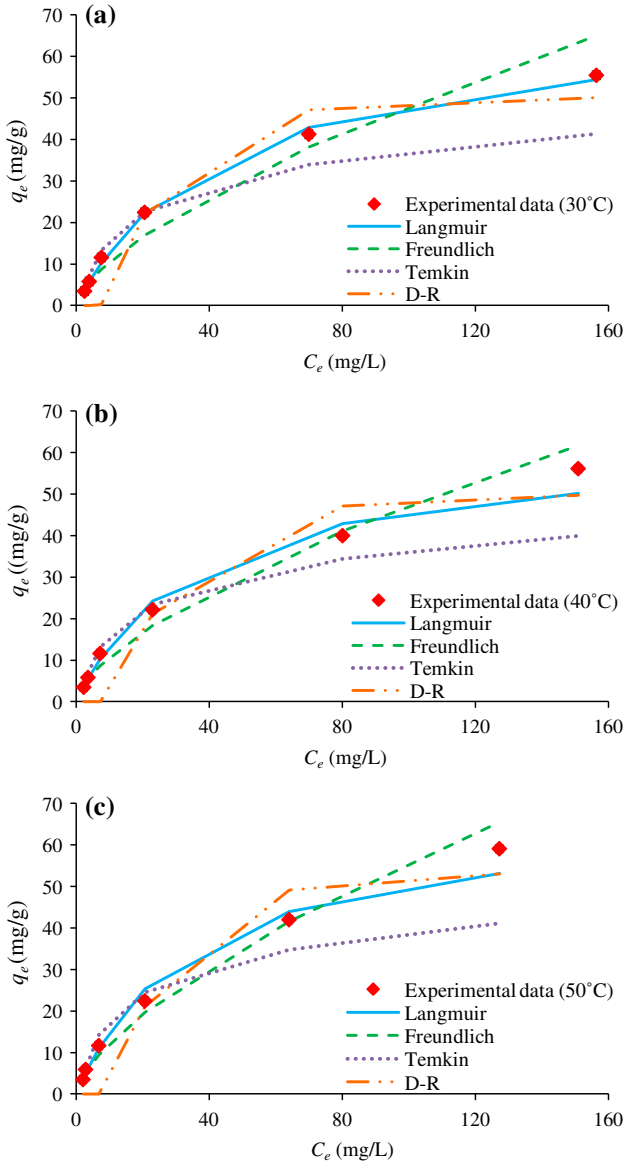

Fig. 3. Comparison of experimental data with theoretical isotherms for MG biosorption onto LAP at 30°C (a), 40°C (b) and 50°C (c).

The interaction between MG and LAP at equilibrium can be described by isotherm models such as Langmuir [37], Freundlich [38], Temkin [39] and Dubinin–Radushkevich (*D–R*) [40]. The respective isotherm equations are listed in Table 1. The experimental data were fitted to these models by non-linear regression method using Microsoft Excel Solver. The degree of fitting of the different models was predicted using the Marquardt's percent standard deviation (*MPSD*)

Table 1
Equilibrium isotherm and kinetic models

Model	Equation	Reference
Langmuir	$q_e = \frac{q_m K_L C_e}{1+K_L C_e}$	[37]
Freundlich	$q_e = K_f C_e^{(1/n_f)}$	[38]
Temkin	$q_e = \frac{RT}{b_T}\ln(K_T C_e)$	[39]
Dubinin–Radushkevich	$q_e = q_s \exp(-\beta\varepsilon^2)$	[40]
Pseudo-first-order kinetic	$q_t = q_e(1 - e^{-k_1 t})$	[42]
Pseudo-second-order kinetic	$q_t = \frac{k_2 t q_e^2}{1+k_2 t q_e}$	[43]
Intraparticle diffusion	$q_t = k_p t^{0.5} + C$	[44]
Marquardt's percent standard deviation (*MPSD*)	$MPSD = 100\sqrt{\frac{1}{n-p}\sum_{i=1}^{N}\left(\frac{q_{e,exp}-q_{e,cal}}{q_{e,exp}}\right)_i^2}$	[45]
Determination coefficient (R^2)	$R^2 = 1 - \frac{\sum_{i=1}^{N}\left(q_{e,\exp}-q_{e,cal}\right)^2}{\sum_{i=1}^{N}\left(q_{e,\exp}-\bar{q}_{e,\exp}\right)^2}$	[45]

Note: Where q_m (mg/g) is the Langmuir maximum sorption capacity, K_L (L/mg) is the Langmuir sorption constant, K_f ((mg/g) (L/mg)$^{1/n}$) is the Freundlich constant, n_f is the Freundlich exponent, b_T (J/mol) is the Temkin constant, K_T (L/mg) is the maximum binding constant, q_s (mg/g) is the *D–R* maximum sorption capacity, β (g^2/J^2) is the activity coefficient, ε (J/g) is the Polanyi potential, k_1 (1/min) is the pseudo-first-order rate constant, k_2 (g/(mg min)) is the pseudo-second-order rate constant, k_P (mg/(g min$^{0.5}$)) is the intraparticle diffusion rate constant, C (mg/g) is the intercept of intraparticle diffusion plot, n is the number of experiments, p is the number of model parameters, and $q_{e,exp}$ (mg/g), $q_{e,cal}$ (mg/g) and $\bar{q}_{e,exp}$ (mg/g) are the experimental, calculated and average experimental equilibrium biosorption capacity, respectively.

and determination coefficient (R^2) (Table 1). Generally, a small *MPSD* and R^2 close to unity indicate good representation of experimental data by the model.

The calculated model parameters are provided along with corresponding *MPSD* and R^2 values in Table 2, while the predicted isotherms are plotted in

Table 2
Isotherm parameters for MG biosorption onto LAP

		Temperature (°C)		
Isotherm model	Model parameters	30	40	50
Langmuir	K_L (L/mg)	0.0230	0.0279	0.0290
	q_m (mg/g)	69.64	62.08	67.54
	R_L	0.0676	0.0563	0.0543
	R^2	0.9975	0.9772	0.9804
	MPSD	7.329	10.301	11.85
Freundlich	K_f (L/mg)	2.299	2.472	2.660
	n_f	1.512	1.559	1.512
	R^2	0.9367	0.9750	0.9774
	MPSD	22.33	18.76	17.33
Temkin	K_T (L/mg)	0.555	0.628	0.707
	b_T (J/mol)	271.7	296.8	294.2
	R^2	0.8834	0.8632	0.8424
	MPSD	22.15	21.18	21.78
D–R	q_s (mg/g)	50.82	50.78	54.38
	β ($\times 10^{-5}$ mol^2/kJ^2):	5.80	7.05	5.83
	R^2	0.8912	0.8753	0.8892
	MPSD	86.63	87.24	87.17

Fig. 3. As can be observed in this figure, the fit of experimental biosorption capacity (q_e) to q_e evaluated using the Langmuir model is noticeably better than to those calculated by the Freundlich, Temkin and *D–R* models. As shown in Table 2, the Langmuir model exhibits lowest *MPSD* (7.329–11.85) and highest R^2 (0.9772–0.9975) suggesting the best fit of data by this model. The Freundlich model also provided reasonable fit to experimental data with quite high R^2 (0.9367–0.9774) and moderately low *MPSD* (17.33–22.33) indicating the suitability of this model. However, when comparing the two models, the Langmuir model is the better model as supported by its lower *MPSD* and higher R^2. Hence, it can be inferred that MG cations were sorbed on homogeneous active sites present in LAP [37]. The Langmuir maximum biosorption capacities (q_m) are between 62.08 and 69.64 mg/g at 30–50˚C. A dimensionless separation factor (R_L) related to the Langmuir model was used to determine whether the biosorption is favourable or unfavourable. It is defined by [41]:

$$R_L = \frac{1}{1 + K_L C_{\max}} \quad (1)$$

where $C_{\max}$ (mg/L) is the highest initial MG concentration. According to theory, the R_L value shows the biosorption as irreversible if $R_L = 0$, favourable if $0 < R_L < 1$ and unfavourable if $R_L > 1$. The calculated R_L varies from 0.0543 to 0.0676 between 30 and 50˚C (Table 2) implying that MG biosorption onto LAP is favourable. The Temkin and *D–R* models did not fit the experimental data well and are inappropriate for describing the biosorption as their R^2 are relatively low and *MSPD* are relatively high.

3.4. Biosorption kinetics

Fig. 4 illustrates the influence of contact time on the biosorption of MG for different initial dye concentrations. There are two distinct biosorption stages: the first one involves a rapid biosorption in which a major fraction of the dye was captured by LAP (0–0.5 min). The second stage involves a slower process whereby equilibrium was achieved after approximately 1 min. The rapid uptake rate at the initial stage could be due to abundant availability of sorption sites. As time progressed, the availability of the sites decreased causing a reduction in the biosorption rate. Fig. 4 also shows that the biosorption capacity of dye increased from 6.57 to 10.54 mg/g when the initial concentration of MG increased from 30 to 50 mg/L. This might be attributed to an increase in driving force for mass transfer when the dye concentration was increased.

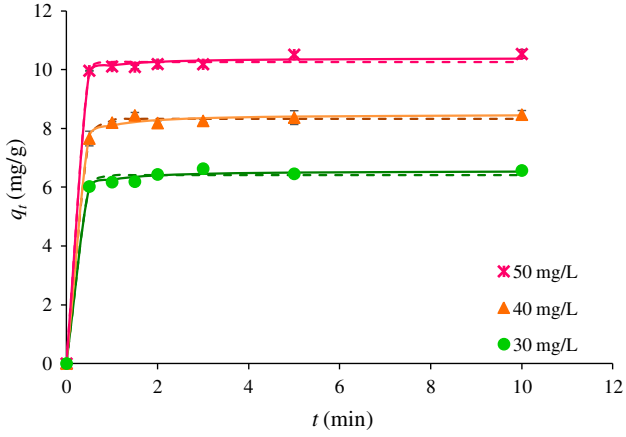

Fig. 4. Comparison of experimental data with data predicted by the pseudo-first-order (dash line) and the pseudo-second-order (solid line) kinetic models for MG biosorption onto LAP.

The goodness-of-fit of experimental data with kinetic models, such as the pseudo-first-order and pseudo-second-order (Table 1), was determined by non-linear curve fitting method. Fig. 4 depicts the comparison of the regressed data for the kinetic models with experimental data at various initial concentrations. The evaluated kinetic parameters, *MPSD* and R^2 values are summarised in Table 3. The parametric values of the pseudo-second-order model are characterised by lower *MPSD* and higher R^2 at most initial concentrations. The q_e evaluated using this model agreed very well with the experimental q_e. The good fit of data by the pseudo-second-order model implies that MG uptake by LAP was mainly by chemisorption, which might involve electron sharing or exchange between the dye and the functional groups in the biosorbent [43]. The initial rates of biosorption ($h_{0,1}$ and $h_{0,2}$) were calculated by [42,43]:

$$h_{0,1} = k_1 q_e \quad (2)$$

$$h_{0,2} = k_2 q_e^2 \quad (3)$$

From Table 3, it can be seen that these rates increase with initial MG concentration. This could be attributed to the increase in driving force for mass transfer of MG with the initial concentration, allowing more dye cations to reach the biosorbent surface in a shorter period of time [46].

Table 3
Kinetic parameters for MG biosorption onto LAP at different initial concentrations

Kinetic model	Model parameters	Initial concentration (mg/L)		
		30	40	50
Pseudo-first-order	$q_{e,\exp}$ (mg/g)	6.569	8.469	10.54
	$h_{o,1}$ (mg/(g min))	35.11	41.70	71.77
	$q_{e,\mathrm{cal}}$ (mg/g)	6.410	8.330	10.27
	k_1 (1/min)	5.478	5.007	6.991
	R^2	0.9952	0.9989	0.9978
	MPSD	2.643	1.275	1.748
Pseudo-second-order	$q_{e,\exp}$ (mg/g)	6.569	8.469	10.54
	$h_{o,2}$ (mg/(g min))	128.7	171.3	391.5
	$q_{e,\mathrm{cal}}$ (mg/g)	6.567	8.496	10.41
	k_2 (g/(mg min))	2.985	2.373	3.615
	R^2	0.9980	0.9985	0.9989
	MPSD	1.698	1.462	1.247

3.5. Biosorption mechanism

In general, the transport of dye from liquid phase to solid biosorbent may occur in several consecutive steps. The overall biosorption process can be limited by one or more steps which include boundary layer (or film) diffusion, intraparticle (or pore) diffusion and sorption on surface sites [47]. To further understand the transport of MG from exterior to internal surfaces, the kinetic data were analysed with the intraparticle diffusion model (Table 1). According to this model, the process is controlled only by intraparticle diffusion if q_t vs. $t^{1/2}$ plot is linear passing through the origin. If the plot is non-linear or linear but does not pass through the origin, then two or more steps may affect the process [44].

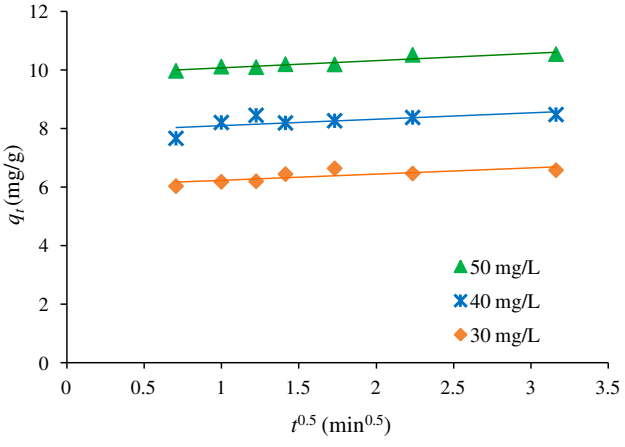

Fig. 5. Plots of intraparticle diffusion model for MG biosorption onto LAP at different initial MG concentrations.

Fig. 5 shows the plots of q_t vs. $t^{1/2}$ for MG biosorption onto LAP at different initial concentrations. None of the plots passes through the origin suggesting that intraparticle diffusion was involved in the process, but not as the sole-limiting step. Instead, the process is limited by several steps such as boundary layer diffusion and intraparticle diffusion. The *y*-intercept of q_t vs. $t^{1/2}$ plot represents the thickness of boundary layer surrounding the biosorbent. Generally, the boundary layer effect will be prominent if the intercept is large. As observed from Fig. 5, the intercept of the plots increases with initial MG concentration. This implies an increase in boundary layer thickness and thus, the greater is the boundary layer effect contribution in the rate-limiting step as initial concentration was increased [48].

3.6. Biosorption thermodynamics

Thermodynamic parameters such as Gibbs free energy change (ΔG°, kJ/mol), enthalpy change (ΔH°, kJ/mol) and entropy change (ΔS°, kJ/(mol K)) were estimated for MG biosorption using:

$$\Delta G^\circ = -RT \log K_C \tag{4}$$

$$\Delta G^\circ = \Delta H^\circ - T\Delta S^\circ \tag{5}$$

where K_C ($=q_e/C_e$) is the distribution coefficient, R (=8.314 J/(mol K)) is the universal gas constant and T

Table 4
Thermodynamic parameters for MG biosorption onto LAP at different initial concentrations.

			ΔG° (kJ/mol) at different temperatures (K)						
C_o (mg/L)	ΔH° (kJ/mol)	ΔS° (J/mol K)	298	303	308	313	318	323	328
30	7.335	−85.0	−18.10	−18.25	−19.27	−19.12	−19.48	−20.04	−20.81
100	0.3319	−63.1	−18.92	−18.49	−18.89	−19.24	−20.03	−20.02	−20.47
200	1.143	−61.7	−17.36	−17.63	−17.78	−17.90	−18.69	−18.79	−19.17
400	12.64	−92.6	−14.28	−16.08	−16.23	−16.18	−16.90	−17.43	−17.48
600	10.40	−82.9	−14.35	−14.80	−15.13	−15.41	−16.05	−16.50	−16.78

(K) is the temperature. The ΔH° and ΔS° values were evaluated from the intercept and slope of the plot of ΔG° vs. T (figure not shown), respectively. The calculated thermodynamic constants are presented in Table 4. The ΔG° values were found to be negative for different temperatures and initial concentrations. This suggests that the process was spontaneous and feasible. In most cases, ΔG° decreased with increasing temperature indicating that the biosorption was more feasible at higher temperatures. Table 4 also displays that ΔH° values are positive implying an endothermic nature of the process. The negative values of ΔS° suggest the decrease in randomness at the solid–liquid interface during the biosorption of MG [18].

4. Conclusions

The efficiency of LAP in removing MG from aqueous solution was evaluated. The maximum biosorption capacity of MG was determined to be 69.64 mg/g at 50℃, dosage 8 g/L and initial pH 4. The equilibrium data were best fitted with the Langmuir model, showing lowest *MPSD* (7.329–11.85) and highest R^2 (0.9772–0.9975) between 30 and 50℃. The kinetic data were represented well by the pseudo-second-order kinetic model which exhibited highest R^2 (0.9980–0.9989) and lowest *MPSD* (1.247–1.698). Thermodynamically, the biosorption of MG onto LAP was endothermic, spontaneous and favourable. Since LAP was used without any pretreatment in the present study, it is an inexpensive and eco-friendly biosorbent with a satisfactory MG biosorption capacity. Therefore, LAP is a potential biosorbent for the removal of MG in aqueous environment.

References

[1] A. Mittal, V. Thakur, J. Mittal, H. Vardhan, Process development for the removal of hazardous anionic azo dye congo red from wastewater by using hen feather as potential adsorbent, Desalin. Water Treat. 52 (2013) 227–237.
[2] S. Chowdhury, P. Saha, Sea shell powder as a new adsorbent to remove basic green 4 (malachite green) from aqueous solutions: Equilibrium, kinetic and thermodynamic studies, Chem. Eng. J. 164 (2010) 168–177.
[3] S. Nausheen, H.N. Bhatti, Z. Furrukh, S. Sadaf, S. Noreen, Adsorptive removal of Drimarine Red HF-3D dye from aqueous solution using low-cost agricultural waste: Batch and column study, Chem. Ecol. 30 (2014) 376–392.
[4] V.K. Gupta, A. Mittal, L. Krishnan, V. Gajbe, Adsorption kinetics and column operations for the removal and recovery of malachite green from wastewater using bottom ash, Sep. Purif. Technol. 40 (2004) 87–96.
[5] A. Mittal, Adsorption kinetics of removal of a toxic dye, malachite green, from wastewater by using hen feathers, J. Hazard. Mater. 133 (2006) 196–202.
[6] O. Hamdaoui, F. Saoudi, M. Chiha, E. Naffrechoux, Sorption of malachite green by a novel sorbent, dead leaves of plane tree: Equilibrium and kinetic modeling, Chem. Eng. J. 143 (2008) 73–84.
[7] S. Chowdhury, P.D. Saha, Scale-up of a dye adsorption process using chemically modified rice husk: Optimization using response surface methodology, Desalin. Water Treat. 37 (2012) 331–336.
[8] S. Srivastava, R. Sinha, D. Roy, Toxicological effects of malachite green, Aquat. Toxicol. 66 (2004) 19–29.
[9] D. Wang, L. Liu, X. Jiang, J. Yu, X. Chen, Adsorption and removal of malachite green from aqueous solution using magnetic β-cyclodextrin-graphene oxide nanocomposites as adsorbents, Colloids Surf. A 466 (2015) 166–173.
[10] A. Mittal, L. Krishnan, V.K. Gupta, Removal and recovery of malachite green from wastewater using an agricultural waste material, de-oiled soya, Sep. Purif. Technol. 43 (2005) 125–133.
[11] S. Chakraborty, S. Chowdhury, P. Das Saha, Adsorption of Crystal Violet from aqueous solution onto NaOH-modified rice husk, Carbohydr. Polym. 86 (2011) 1533–1541.
[12] J. Mittal, D. Jhare, H. Vardhan, A. Mittal, Utilization of bottom ash as a low-cost sorbent for the removal and recovery of a toxic halogen containing dye eosin yellow, Desalin. Water Treat. 52 (2013) 4508–4519.
[13] J. Mittal, V. Thakur, A. Mittal, Batch removal of hazardous azo dye Bismark Brown R using waste material hen feather, Ecol. Eng. 60 (2013) 249–253.
[14] S. Sadaf, H.N. Bhatti, S. Ali, K-u. Rehman, Removal of Indosol Turquoise FBL dye from aqueous solution by bagasse, a low cost agricultural waste: Batch and column study, Desalin. Water Treat. 52 (2013) 184–198.

[15] H. Daraei, A. Mittal, M. Noorisepehr, F. Daraei, Kinetic and equilibrium studies of adsorptive removal of phenol onto eggshell waste, Environ. Sci. Pollut. Res. 20 (2013) 4603–4611.
[16] P. King, N. Rakesh, S.B. Lahari, Y.P. Kumar, V.S.R.K. Prasad, Biosorption of zinc onto *Syzygium cumini* L.: Equilibrium and kinetic studies, Chem. Eng. J. 144 (2008) 181–187.
[17] E.C. Lima, B. Royer, J.C.P. Vaghetti, N.M. Simon, B.M. da Cunha, F.A. Pavan, E.V. Benvenutti, R. Cataluña-Veses, C. Airoldi, Application of Brazilian pine-fruit shell as a biosorbent to removal of reactive red 194 textile dye from aqueous solution: Kinetics and equilibrium study, J. Hazard. Mater. 155 (2008) 536–550.
[18] S. Nawaz, H.N. Bhatti, T.H. Bokhari, S. Sadaf, Removal of Novacron Golden Yellow dye from aqueous solutions by low-cost agricultural waste: Batch and fixed bed study, Chem. Ecol. 30 (2013) 52–65.
[19] L.P.Y. Foo, C.Z. Tee, N.R. Raimy, D.G. Hassell, L.Y. Lee, Potential Malaysia agricultural waste materials for the biosorption of cadmium(II) from aqueous solution, Clean Technol. Environ. 14 (2011) 273–280.
[20] M. Fomina, G.M. Gadd, Biosorption: Current perspectives on concept, definition and application, Bioresour. Technol. 160 (2014) 3–14.
[21] X. Han, J. Yuan, X. Ma, Adsorption of malachite green from aqueous solutions onto lotus leaf: Equilibrium, kinetic, and thermodynamic studies, Desalin. Water Treat. 52 (2013) 5563–5574.
[22] A. Witek-Krowiak, Biosorption of malachite green from aqueous solutions by pine sawdust: Equilibrium, kinetics and the effect of process parameters, Desalin. Water Treat. 51 (2013) 3284–3294.
[23] S. Sadaf, H.N. Bhatti, Batch and fixed bed column studies for the removal of Indosol Yellow BG dye by peanut husk, J. Taiwan Inst. Chem. Eng. 45 (2014) 541–553.
[24] L.Y. Lee, D.Z.B. Chin, X.J. Lee, N. Chemmangattuvalappil, S. Gan, Evaluation of *Abelmoschus esculentus* (lady's finger) seed as a novel biosorbent for the removal of Acid Blue 113 dye from aqueous solutions, Process Saf. Environ. (2014), doi: 10.1016/j.psep.2014.08.004.
[25] S. Chowdhury, S. Chakraborty, P. Saha, Biosorption of Basic Green 4 from aqueous solution by *Ananas comosus* (pineapple) leaf powder, Colloids Surf. B 84 (2011) 520–527.
[26] I.J. Bulbul, A.H.M. Zulfiker, K. Hamid, M.H. Khatun, Y. Begum, Comparative study of *in vitro* antioxidant, antibacterial and cytotoxic activity of two Bangladeshi medicinal plants—*Luffa cylindrica* L. and *Luffa acutangula*, Pharmacognosy J. 3 (2011) 59–66.
[27] L.Y. Lee, X.J. Lee, P.C. Chia, K.W. Tan, S. Gan, Utilisation of *Cymbopogon citratus* (lemon grass) as biosorbent for the sequestration of nickel ions from aqueous solution: Equilibrium, kinetic, thermodynamics and mechanism studies, J. Taiwan Inst. Chem. Eng. 45 (2014) 1764–1772.
[28] S. Sadaf, H. Bhatti, Evaluation of peanut husk as a novel, low cost biosorbent for the removal of Indosol Orange RSN dye from aqueous solutions: Batch and fixed bed studies, Clean Technol. Environ. 16 (2014) 527–544.
[29] V.S. Mane, I.D. Mall, V.C. Srivastava, Use of bagasse fly ash as an adsorbent for the removal of brilliant green dye from aqueous solution, Dyes Pigm. 73 (2007) 269–278.
[30] Y.-C. Lee, M. Choi, J.-W. Yang, H.-J. Shin, Removal of malachite green (MG) from aqueous solutions by adsorption, precipitation, and alkaline fading using talc: Kinetic, thermodynamic, and column feasibility studies, Desalin. Water Treat. (2014) 1–11.
[31] I.D. Mall, V.C. Srivastava, N.K. Agarwal, I.M. Mishra, Adsorptive removal of malachite green dye from aqueous solution by bagasse fly ash and activated carbon-kinetic study and equilibrium isotherm analyses, Colloids Surf. A 264 (2005) 17–28.
[32] M.-H. Baek, C.O. Ijagbemi, S.-J. O, D.-S. Kim, Removal of Malachite Green from aqueous solution using degreased coffee bean, J. Hazard. Mater. 176 (2010) 820–828.
[33] H. Chen, J. Zhao, G. Dai, Silkworm exuviae-A new non-conventional and low-cost adsorbent for removal of methylene blue from aqueous solutions, J. Hazard. Mater. 186 (2011) 1320–1327.
[34] N. Barka, K. Ouzaouit, M. Abdennouri, M.E. Makhfouk, Dried prickly pear cactus (*Opuntia ficus indica*) cladodes as a low-cost and eco-friendly biosorbent for dyes removal from aqueous solutions, J. Taiwan Inst. Chem. Eng. 44 (2013) 52–60.
[35] B.H. Hameed, M.I. El-Khaiary, Batch removal of malachite green from aqueous solutions by adsorption on oil palm trunk fibre: Equilibrium isotherms and kinetic studies, J. Hazard. Mater. 154 (2008) 237–244.
[36] E.W. Baumann, Colorimetric determination of low pH with Malachite Green, Talanta 42 (1995) 457–462.
[37] I. Langmuir, The adsorption of gases on plane surfaces of glass, mica and platinum, J. Am. Chem. Soc. 40 (1918) 1361–1403.
[38] H.M.F. Freundlich, Über die adsorption in lösungen (Over the adsorption in solution), J. Phys. Chem. 57 (1906) 385–470.
[39] M.I. Temkin, V.M. Pyzhev, Kinetics of ammonia synthesis on promoted iron catalyst, Acta Physiochim. USSR 12 (1940) 327–356.
[40] M.M. Dubinin, L.V. Radushkevich, The equation of the characteristic curve of the activated charcoal, Proc. Acad. Sci. USSR 55 (1947) 331–333.
[41] K.R. Hall, L.C. Eagleton, A. Acrivos, T. Vermeulen, Pore- and solid-diffusion kinetics in fixed-bed adsorption under constant-pattern conditions, Ind. Eng. Chem. Fundam. 5 (1966) 212–223.
[42] S. Lagergren, About the theory of so-called adsorption of soluble substances, K. Sven. Vetensk. Handl. 24 (1989) 1–39.
[43] Y.S. Ho, G. McKay, Sorption of dye from aqueous solution by peat, Chem. Eng. J. 70 (1998) 115–124.
[44] W.J. Weber, J.C. Morris, Kinetics of adsorption on carbon from solution, J. Sanitary Eng. Div. Am. Soc. Civ. Eng. 89 (1963) 31–59.
[45] D.C. Montgomery, Design and Analysis of Experiments, Wiley, New York, NY, 2011.

[46] W. Cheng, S.-G. Wang, L. Lu, W.-X. Gong, X.-W. Liu, B.-Y. Gao, H.-Y. Zhang, Removal of malachite green (MG) from aqueous solutions by native and heat-treated anaerobic granular sludge, Biochem. Eng. J. 39 (2008) 538–546.
[47] X.J. Lee, L.Y. Lee, L.P.Y. Foo, K.W. Tan, D.G. Hassell, Evaluation of carbon-based nanosorbents synthesised by ethylene decomposition on stainless steel substrates as potential sequestrating materials for nickel ions in aqueous solution, J. Environ. Sci. 24 (2012) 1559–1568.
[48] V.S. Mane, P.V. Vijay Babu, Kinetic and equilibrium studies on the removal of Congo red from aqueous solution using Eucalyptus wood (*Eucalyptus globulus*) saw dust, J. Taiwan Inst. Chem. Eng. 44 (2013) 81–88.